

Modelling the Light Scattering Behavior of Transmission-Mode GaAs Photocathode Under the AlGaAs Window Layer Rough Surface

Xin Guo[✉], Feng Shi[✉], Tiantian Jia, Ruoyu Zhang, Jinjuan Du, Peng Chen, Haoyu Wu, Hongchang Cheng, and Yijun Zhang

Abstract—To improve the understanding of the optical image resolution of transmission-mode GaAs photocathode, by establishing the surface scattering analysis model of AlGaAs window layer, we have researched the effect of the surface height distribution variance σ on scattering surface transfer function (STF) and point spread function (PSF) of transmission-mode GaAs photocathode. The simulation results show that the decrease of surface height distribution variance σ is beneficial to improve the optical image resolution. This improvement is mainly attributed to the decrease in input light energy attenuation and spatial diffusion caused by smaller surface height distribution variance σ , and thus the signal to noise ratio of scattering degraded optical image is increased.

Index Terms—AlGaAs window layer, GaAs photocathodes, point spread function, scattering surface transfer function.

I. INTRODUCTION

NOWADAYS, III-V negative electron affinity semiconductor photocathode technology plays an increasingly important role in low illumination detection for various applications including night vision, vacuum electron source and high-speed photography [1], [2], [3], [4], [5]. As far as the field of night vision is concerned, the imaging quality level can be directly and quickly reflected through the integral sensitivity and limited resolution [6], [7]. The integral sensitivity can be used to describe the photoelectric conversion efficiency of the transmission-GaAs photocathode, which directly affects the lowest detection

Manuscript received 15 February 2023; revised 8 March 2023; accepted 9 March 2023. Date of publication 14 March 2023; date of current version 23 March 2023. This work was supported in part by the National Natural Science Foundation of China under Grants 61771245 and 62271259 and in part by the Defense Industrial Technology Development Program of China under Grant JCKY2018208B016. (*Corresponding authors:* Xin Guo; Feng Shi.)

Xin Guo and Feng Shi are with the School of Optoelectronics, Beijing Institute of Technology, Beijing 100081, China, and also with the Science and Technology on Low-Light-Level Night Version Laboratory, Xi'an 710065, China (e-mail: guoxinkakaxi@126.com; zhifengxu_ok@163.com).

Tiantian Jia, Ruoyu Zhang, Jinjuan Du, Peng Chen, Haoyu Wu, and Hongchang Cheng are with the Science and Technology on Low-Light-Level Night Version Laboratory, Xi'an 710065, China (e-mail: j936435988@163.com; zhangruoyu19020220@gmail.com; jinjuan5826@163.com; 13679130895@163.com; 17636471316@163.com; chh600@163.com).

Yijun Zhang is with the School of Electronic and Optical Engineering, Nanjing University of Science and Technology, Nanjing 210094, China (e-mail: zhangyijun423@126.com).

Digital Object Identifier 10.1109/JPHOT.2023.3256699

illuminance. Besides the integral sensitivity, the limited resolution is also quite important in low illumination detection research [8]. By analyzing the limited resolution, the detail resolution of the image can be provided [9]. Particularly, transmission-mode GaAs photocathode has been extensively developed in the field of low-light-level imaging due to the high quantum efficiency, small dark emission, adjustable long-wave threshold, and large long-wave response expansion potential [10], [11], [12], [13]. Therefore, for real-time night vision, it is necessary to consider the integral sensitivity, limited resolution, response time and other requirements of transmission-mode GaAs photocathode at the same time.

For a transmission-mode GaAs photocathode, the input light must pass through the window glass and AlGaAs window layer first and then be absorbed by the GaAs photoemission layer and converted into electron image [14]. So both the optical image resolution and electron image resolution of GaAs photocathode are major considerations. Whereas most research into GaAs photocathode has focused on how to improve its electron image resolution, and very little research has focused on improving its optical image resolution [15], [16], [17]. Deng et al established the electron image resolution model and modulation transfer function (MTF) of varying doping and varying composition GaAs photocathode in 2022 [15]. Wang et al have researched the effect of electron lateral diffusion in transmission -mode varied-doping Al_{0.37}Ga_{0.63}N photocathode on resolution in 2022 [16]. Theoretical research showed that the inhibition on lateral diffusion of electrons is beneficial to improve the electron image resolution of GaAs photocathode, caused by an appropriate electric field or reasonably designed photocathode parameters. However, it is hard to further improve the resolution of GaAs photocathode. In practice, during the transmission of input light, some deterioration of optical image resolution is bound to occur in GaAs photocathode. The input light scatters on the rough surface of the AlGaAs window layer, which weakens the energy of the optical image and degrades the image quality [18], [19]. As a result, the light scattering behavior in GaAs photocathode accounts for this deterioration. Under this direction and according to high resolution GaAs photocathode requirements, it is important to discuss the effect of the light scattering behavior in GaAs photocathode on resolution.

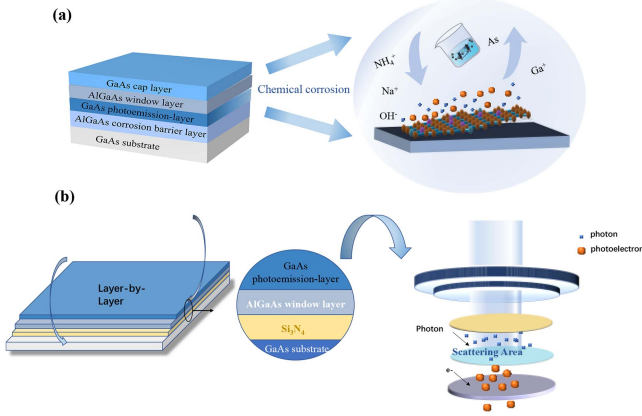


Fig. 1. (a) Structural schematic of GaAs photocathode material. (b) Schematic diagram of the light scattering principle from the rough surface of AlGaAs window layer in the transmission-mode GaAs photocathode.

Therefore, in the work of this paper, due to the lack of theoretical models for the analysis of the light scattering behavior in transmission-mode GaAs photocathode, an AlGaAs window layer scattering analysis model based on scattering surface transfer function (STF) is proposed. We simulated the differences of STF and point spread function (PSF) for different surface roughness at the same input light wavelength. In addition, the degradation degree of optical image caused by the light scattering of AlGaAs window layer was analyzed by using the peak signal-to-noise ratio (PSNR), so as to study the influence of different surface roughness of AlGaAs window layer on the optical image resolution of GaAs photocathode. This research provides a possible way to improve the resolution performance of transmission-mode GaAs photocathode.

II. MODEL AND DETAILS

Fig. 1(a) is a simple structural schematic of GaAs photocathode material. GaAs photocathode material adopts multi-layer heterogeneous epitaxial structure, which mainly includes GaAs substrate, 50 μm -thick Al_{0.3}Ga_{0.7}As corrosion barrier layer, 1.5 μm -thick GaAs photoemission layer, 0.5 μm -thick Al_{0.7}Ga_{0.3}As window layer and 0.1 μm -thick GaAs cap layer. The aim of designing GaAs gap layer is mainly to avoid the possible chemical contamination and mechanical damage of GaAs photocathode material. In the preparation of the transmission-mode GaAs photocathode, a wet chemical etching method is required to remove the GaAs cap layer to expose the AlGaAs window layer. Therefore, the surface of the AlGaAs window layer is inevitably rough. An optical antireflective film is manufactured on the surface of the rough AlGaAs window layer and bonded with the window glass to basically complete the preparation of the transmission-mode GaAs photocathode. Due to the existence of a certain surface roughness of the AlGaAs window layer, the input light is bound to scatter on the surface of the AlGaAs window layer, thus reducing the resolution of the optical image, as shown in Fig. 1(b).

Assuming that the rough surface of AlGaAs window layer is random [20], the height obeys Gaussian distribution and the

light of incidence should be vertical, the STF is defined as [21]

$$\text{STF} = \exp \left\{ -(4\pi\sigma)^2 \left| 1 - \frac{\text{ACV}(\bar{x}, \bar{y})}{\sigma^2} \right| \right\} \quad (1)$$

Where $\text{ACV}(\bar{x}, \bar{y})$ is two-dimensional surface autocorrelation function, σ is surface height distribution variance, λ is wavelength of incident light, \bar{x} equals x/λ , \bar{y} equals y/λ .

In order to comprehensively describe the rough surface of the AlGaAs window layer and characterize the optical surface quality in a certain spatial frequency scale range, an optical power spectral density function (PSD) [22], [23] is determined by

$$\text{PSD}_{(f_x, f_y)}$$

$$= \left| \frac{1}{l_x l_y} \iint h(x, y) \exp[-i(f_x x + f_y y)] df_x df_y \right|^2 \quad (2)$$

Where $h(x, y)$ is the optical surface profile vector height distribution, representing the undulation of the surface profile, l_x and l_y stand for the autocorrelation lengths in two vertical directions, respectively. Specially, $h(x, y)$ is given by [24]

$$h(x, y) = \frac{1}{2\pi\sigma^2} \exp \left(-\frac{x^2 + y^2}{2\sigma^2} \right) \quad (3)$$

Subsequently, by solving (2) for PSD (f_x, f_y) and performing inverse Fourier transformation, $\text{ACV}(\bar{x}, \bar{y})$ can be obtained and it is given by [25]

$$\text{ACV}(\bar{x}, \bar{y}) = \sigma^2 \left(1 / \exp \left(\frac{x/\lambda}{l_x^2} + \frac{y/\lambda}{l_y^2} \right) \right) \quad (4)$$

More specially, substituting (4) into (1), we can establish this model as

$$\text{STF}_{\text{AlGaAs}} = \exp \left\{ -(4\pi\sigma)^2 \left| 1 - \exp \left(\frac{x}{\lambda l_x^2} + \frac{y}{\lambda l_y^2} \right) \right| \right\} \quad (5)$$

III. RESULTS AND DISCUSSIONS

A. Surface Morphology of AlGaAs Window Layer

In order to study the influence of light scattering behavior in transmission-mode GaAs photocathode on the optical image resolution, we simulated the surface morphology of AlGaAs window layer under different roughness. Assuming that the autocorrelation lengths in both x and y directions in the AlGaAs window layer are l_c , the surface pattern distribution of the AlGaAs window layer can be calculated as [26]

$$Z(x, y) = h(x, y) * g(x, y) \quad (6)$$

Where $g(x, y)$ denotes the Gaussian filter function and is given by [27]

$$g(x, y) = \frac{2\sigma}{\sqrt{\pi l_c}} \exp \left(-2 \frac{x^2 + y^2}{l_c^2} \right) \quad (7)$$

Assuming that $l_c = 3$, and $\sigma = 0.1 \text{ nm}$, 0.5 nm and 1 nm , respectively, the surface morphologies of AlGaAs window layer are shown in Fig. 2. Clearly, it is found that surface undulation of AlGaAs window layer rise dramatically with increasing the surface height standard deviation distribution σ . For instance, the

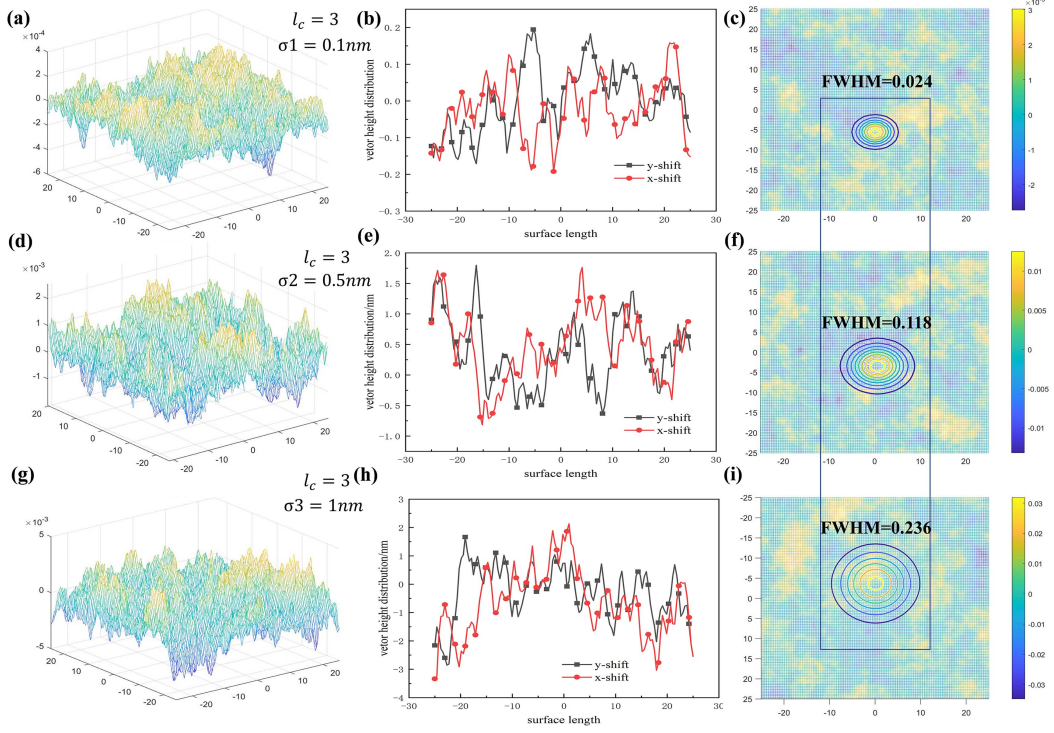


Fig. 2. (a) $\sigma_1 = 0.1$ nm, $l_c = 3$, three-dimensional Gaussian rough surface; (b) $\sigma_1 = 0.1$ nm, $l_c = 3$, one-dimensional Gaussian rough surface numerical distribution; (c) $\sigma_1 = 0.1$ nm, $l_c = 3$, Gaussian rough surface FWHM contour distribution; (d) $\sigma_2 = 0.5$ nm, $l_c = 3$, three-dimensional Gaussian rough surface; (e) $\sigma_2 = 0.5$ nm, $l_c = 3$, one-dimensional Gaussian rough surface numerical distribution; (f) $\sigma_2 = 0.5$ nm, $l_c = 3$, Gaussian rough surface FWHM contour distribution; (g) $\sigma_3 = 1$ nm, $l_c = 3$, three-dimensional Gaussian rough surface; (h) $\sigma_3 = 1$ nm, $l_c = 3$, one-dimensional Gaussian rough surface numerical distribution; (i) $\sigma_3 = 1$ nm, $l_c = 3$, Gaussian rough surface FWHM contour distribution.

peak-to-valley difference of AlGaAs rough surface are 5.5 nm and 0.35 nm for $\sigma = 1$ nm and 0.1 nm, respectively, i.e., it increases by an order of magnitude. In addition, according to the distribution of simulated Gaussian surface rough points, the full width at half maximum (FWHM) value increased with the increase of standard deviation value, from 0.024 nm to 0.236 nm, indicating that the surface rough point not only increased the degree of height undulation, but also the degree of discreteness of the rough point. From the standpoint of input transport, When the input light passes through the rough surface of AlGaAs window layer, the input light will deviate from the original propagation direction, so that the input light will be redistributed spatially, and the intensity of the input light in the original propagation direction will be weakened. Particularly, for a given transmission-mode GaAs photocathode, the weakening of optical image energy leads to a reduction in imaging quality.

B. Surface Transfer Function and Point Spread Function

In a bid to research the effect of the surface height standard deviation distribution σ on STF and PSF of transmission-mode GaAs photocathodes, we give STF and PSF in the case of $\lambda = 800$ nm, via changing $\sigma = 0.1$ nm, 0.5 nm and 1 nm, individually. As shown in Fig. 3, it is clear that the lower σ leads to higher STF. Moreover, the area surrounded by STF two-dimensional curve is calculated. As σ decreases, the area (dimensionless) surrounded by STF increases from 116 to 180.

Stated another way, the lower σ can give rise to the optical image resolution. This phenomenon is attributed to the fact that the reduction of STF means that the area or integral value enclosed by the surface transfer function is smaller, that is, the smaller the capacity of optical image information and the more blurred the imaging.

The PSF of AlGaAs window layer rough surface can be obtained by Fourier quasi-transform based on the scattering surface transfer function, as follows:

$$\begin{aligned} & PSF(f_x, f_y) \\ &= \int_{-\infty}^{+\infty} \int_{-\infty}^{+\infty} H(\hat{x}, \hat{y}) e^{i2\pi(\hat{x}f_x + \hat{y}f_y)} dx dy \end{aligned} \quad (8)$$

By assuming $\sigma = 0.1$ nm, 0.5 nm and 1 nm, The PSF of AlGaAs window layer rough surface haven been shown in Fig. 4. As can be seen form Fig. 4, it is obvious that the central value of PSF fall as the surface height standard deviation distribution σ is increased, which indicates that the central energy of the input optical image decreases. In addition, in the small range outside the center of the PSF, its value rises with the increase of the surface height standard deviation distribution σ . More specially, the rate of decrease in the value of the PSF rises more markedly as $\sigma = 0.1$ nm. It is well illustrated by the fact that the input image energy is shifted outward with increasing surface height standard deviation distribution and produces a spot with increased brightness and slightly smaller brightness range. In the

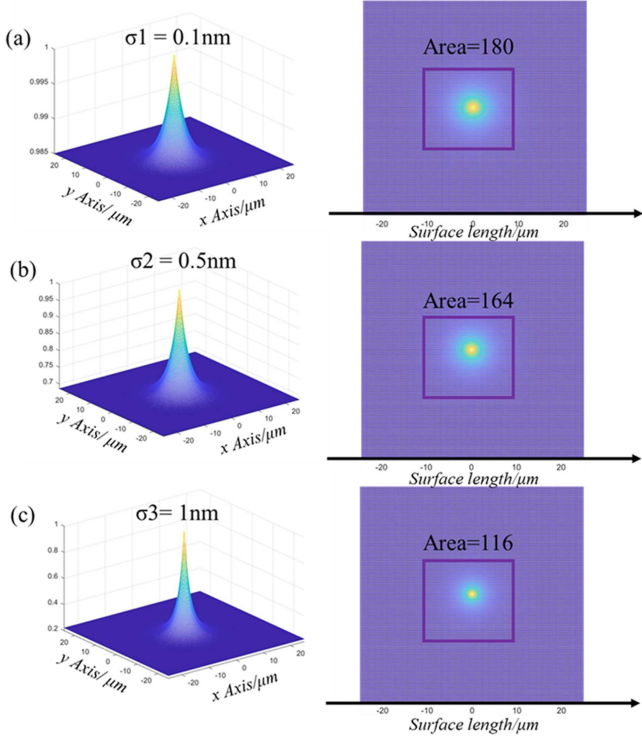


Fig. 3. (a) STF function of $\sigma_1 = 0.1 \text{ nm}$, $l_c = 3$, left: three-dimensional STF, right: two-dimensional STF; (b) STF function of $\sigma_2 = 0.5 \text{ nm}$, $l_c = 3$, left: three-dimensional STF, right: two-dimensional STF; (c) $\sigma_3 = 1 \text{ nm}$, $l_c = 3$, left: three-dimensional STF, right: two-dimensional STF.

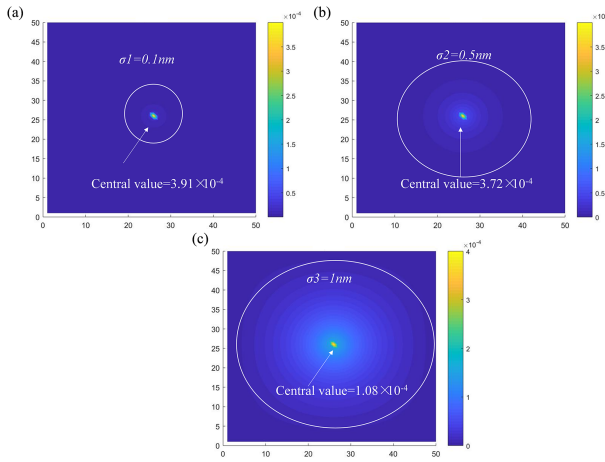


Fig. 4. Point diffusion function of different rough surfaces: (a) $\sigma_1 = 0.1 \text{ nm}$ (b) $\sigma_2 = 0.5 \text{ nm}$ (c) $\sigma_3 = 1 \text{ nm}$.

meanwhile, as the surface height standard deviation distribution σ increases, the PSF produces more fluctuations at the edges, and thus the energy edge distribution of the input optical image becomes more unstable as a result of higher surface height standard deviation distribution.

As discussed above, there is an obvious qualitative and quantitative relationship between the STF and PSF values of the rough surface of the AlGaAs window layer. The increase of the surface height distribution variance of the AlGaAs window layer will reduce the STF and the PSF, so that the input optical image

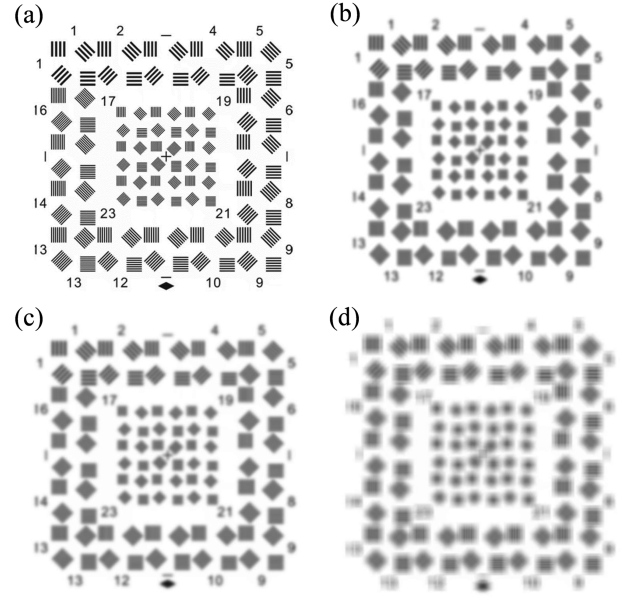


Fig. 5. Degradation of signal-to-noise ratio for rough surface imaging with different standard deviation distributions: (a) original (b) $\sigma_1 = 0.1 \text{ nm}$ (c) $\sigma_2 = 0.5 \text{ nm}$ (d) $\sigma_3 = 1 \text{ nm}$.

energy is reduced and the input optical energy distribution is not centralized. Therefore, the optical image resolution of the transmission-mode GaAs photocathode will be decreased.

C. Signal to Noise Ratio of Scattering Degraded Image

In order to analyze the influence of optical image quality of input light scattering on the AlGaAs window layer rough surface, the PSF with varying surface height distribution variance σ are convolved with the original image of a given standard resolution target to simulate image degradation, as shown in Fig. 5(a)–(d). It can be observed from Fig. 5(a)–(d) that with the increase of surface height standard deviation distribution variance σ , the optical image quality significantly decreases.

In order to realize the quantitative analysis of the optical image degradation degree corresponding to the scattering of different surface height standard deviation distribution variance σ on the AlGaAs rough surface window layer, the optical image quality is evaluated by using the parametric mean square error and parametric peak signal-to-noise ratio. The formulas of parametric mean square error and parametric peak signal-to-noise ratio are as follows [28], [29]:

$$MSE_R = \frac{\sum_{i=1}^M \sum_{j=1}^N \left[f(i, j) - \hat{f}(i, j) \right]^2}{N \times M} \quad (9)$$

$$\begin{aligned} PSNR_R &= 10 \log_{10} \frac{K^2}{MSE_R} \\ &= 10 \log_{10} \frac{N \times M \times K^2}{\sum_{i=1}^M \sum_{j=1}^N \left[f(i, j) - \hat{f}(i, j) \right]^2} \end{aligned} \quad (10)$$

TABLE I
PSNR OF DEGRADED IMAGE WITH DIFFERENT INCIDENT LIGHT WAVELENGTHS

Models	0.1nm	0.5nm	1nm
PSNR	18.91	18.35	17.58

Where $f(i, j)$ is original image, $\hat{f}(x, y)$ is degraded image, $N \times M$ is image size, K is quantization bits of digital images.

Table I is the correspondence table between different surface height standard deviation distribution variance σ and the parametric peak signal-to-noise ratio after image degradation. It can be seen from the table that the surface height standard deviation distribution variance σ increases from 0.1 nm to 1 nm, and the parametric peak signal-to-noise ratio after image degradation can be decreased from 18.91 to 17.98. At this point, the degree of optical image quality degradation due to different surface height distribution variance is different, that is, the reduction of the surface height distribution variance helps to narrow the gap between the degraded image quality and the original image quality, thus improving the resolution of optical image. In practical application, the surface height distribution variance σ of the AlGaAs window layer must be continuously reduced to mitigate the degradation of optical image quality caused by the scattering of input light on the AlGaAs window layer rough surface, so as to obtain a high-resolution transmission-mode GaAs photocathode.

V. CONCLUSION

In conclusion, the scattering of input light on the AlGaAs window layer rough surface is one of the main reasons for the degradation in the optical image resolution of a transmission-mode GaAs photocathode. The surface height distribution σ of the AlGaAs window layer is a very critical parameter affecting the scattering behavior of input light, thus a surface scattering analysis model of AlGaAs window layer based on scattering transfer function is established. The effect of surface height distribution σ on the optical image resolution of transmission-mode GaAs photocathode was discussed by calculating and comparing STF and PSF. The simulation results show that the area enclosed by the STF is the largest and the signal-to-noise ratio of the image after scattering degradation is the highest when the surface height distribution σ is 0.1 nm compared to 1 nm, which indicates that the input optical image has the smallest energy loss, the highest information capacity and the best image quality. The results in this paper could provide some references for exploring the improvement of high-resolution transmission-mode GaAs photocathode.

REFERENCES

- [1] K. Chrzanowski, "Review of night vision technology," *Opto-Electron. Rev.*, vol. 21, pp. 153–181, 2013.
- [2] J.-W. Schwede et al., "Photon-enhanced thermionic emission from heterostructures with low interface recombination," *Nature Commun.*, vol. 4, 2013, Art. no. 1576.
- [3] K. Mitsuno et al., "Activation process of GaAs NEA photocathode and its spectral sensitivity," in *Proc. 3rd Int. Conf. Nanotechnol. Biomed. Eng.*, 2016, pp. 163–166.
- [4] M. Kuwahara et al., "30-kV spin-polarized transmission electron microscope with GaAs-GaAsP strained superlattice photocathode," *Appl. Phys. Lett.*, vol. 101, 2012, Art. no. 033102.
- [5] J.-K. Bae et al., "Rugged spin-polarized electron sources based on negative electron affinity GaAs photocathode with robust Cs₂Te coating," *Appl. Phys. Lett.*, vol. 112, 2018, Art. no. 154101.
- [6] J.-M. Medina, " $1/f^\alpha$ noise in reaction times: A proposed model based on Pieron's law and information processing," *Phys. Rev. E*, vol. 79, no. 1, 2009, Art. no. 011902.
- [7] D.-G. Fisher et al., "Negative electron affinity materials for imaging devices," *Adv. Image Pickup Display*, vol. 1, pp. 101–106, 1974.
- [8] L. Ren et al., "Modulation transfer function characteristic of uniform-doping transmission-mode GaAs/GaAlAs photocathode," *Chin. Phys. B*, vol. 20, no. 8, 2011, Art. no. 087308.
- [9] W.-J. Deng et al., "Resolution characteristics of graded band-gap reflection-mode AlGaAs/GaAs photocathodes," *Opt. Commun.*, vol. 356, pp. 278–281, 2015.
- [10] X.-G. Jin et al., "Mean transverse energy and response time measurements of GaInP based photocathodes," *J. Appl. Phys.*, vol. 116, 2014, Art. no. 064501.
- [11] S. Uchiyama et al., "GaN-based photocathodes with extremely high quantum efficiency," *Appl. Phys. Lett.*, vol. 86, 2005, Art. no. 103511.
- [12] D. A. Orlov et al., "Long term operation of high quantum efficiency GaAs (Cs, O) photocathodes using multiple recleaning by atomic hydrogen," *J. Appl. Phys.*, vol. 106, 2009, Art. no. 54907.
- [13] B.-K. Chang et al., "Spectral response and surface layer thickness of GaAs: Cs-O negative electron affinity photo-cathode," *Proc. SPIE*, vol. 4580, pp. 632–641, 2001.
- [14] J. P. André, P. Guittard, J. Hallais, and C. Piaget, "GaAs photocathodes for low light level imaging," *J. Cryst. Growth*, vol. 55, pp. 255–245, 1981.
- [15] W.-J. Deng et al., "Resolution characteristics of varying doping and varying composition Al_xGa_{1-x}As/GaAs reflective photocathodes," *Acta Physica Sinica*, vol. 71, no. 15, 2022, Art. no. 157901.
- [16] H.-G. Wang et al., "Effect of lateral diffusion of photoelectrons in the reflection-mode varied-doping AlGaN photocathode on resolution," *Appl. Opt.*, vol. 60, no. 25, pp. 7658–7663, 2021.
- [17] W.-J. Deng et al., "Resolution characteristic of graded band-gap Al-GaAs/GaAs transmission-mode photocathodes," *Acta Physica Sinica*, vol. 63, no. 16, 2014, Art. no. 167902.
- [18] T.-F. Qiu et al., "Resolution research of low-light-level image intensifier based on electronic trajectory tracking," *Acta Photonica Sinica*, vol. 49, no. 12, 2020, Art. no. 1223003.
- [19] W.-J. Deng et al., "Resolution characteristics of varying doping and varying composition Al_xGa_{1-x}As/GaAs reflective photocathodes," *Acta Physica Sinica*, vol. 71, no. 15, 2022, Art. no. 157901.
- [20] A. Krywonos, "Predicting surface scatter using a linear systems formulation of non-paraxial scalar diffraction," Univ. Central Florida, Orlando, FL, USA, 2006.
- [21] J.-E. Harvey, "Integrating optical fabrication and metrology into the optical design process," *Appl. Opt.*, vol. 54, no. 9, pp. 2224–2233, 2015.
- [22] E.-I. Thorsos, "The validity of the Kirchhoff approximation for rough surface scattering using a Gaussian roughness spectrum," *J. Acoustical Soc. Amer.*, vol. 83, pp. 78–92, 1988.
- [23] K.-M. Aamir et al., "Recursive Wiener-Khintchine theorem," *Int. J. Comput., Elect., Automat., Control Inf. Eng.*, 2004.
- [24] J.-E. Harvey et al., "Scattering effects from residual optical fabrication errors," *Proc. SPIE*, vol. 2576, pp. 155–174, 1995.
- [25] N.-V. Manuel et al., "A detailed study of the scattering of scalar waves from random rough surface," *Optica Acta: Int. J. Opt.*, vol. 28, no. 12, pp. 1651–1672, 1981.
- [26] E.-L. Church, "Fractal surface finish," *Appl. Opt.*, vol. 27, no. 8, pp. 1518–1526, 1988.
- [27] X.-F. Zeng, "Effect of optical surface frequency band error on imaging quality," Graduate Univ. Chin. Acad. Sci. (Changchun Inst. Opt., Fine Mechanics Phys.), 2014.
- [28] J. Zhao et al., "Improved edge-guided network for single image super-resolution," *Multimedia Tools Appl.*, vol. 81, no. 1, pp. 343–365, 2022.
- [29] Q.-X. Liu et al., "Modified Remora optimization algorithm for global optimization and multilevel thresholding image segmentation," *Mathematics*, vol. 10, no. 7, 2022, Art. no. 1014.